AD-A266 804

# UMENTATION PAGE

Form Approved
OMB No. 0704-0188



| 2. REPORT DATE | 3. REPORT TYPE AND DATES COVERED |
|---|---|
| 4/30/93 | Final 1 Jul 92 - 1 Apr 93 |

**4. TITLE AND SUBTITLE**

A Novel Solid-State Optical Temporal Analyzer with Picosecond Resolution and Picowatt Sensitivity

**5. FUNDING NUMBERS**

DAAL03-92-C-0035

**6. AUTHOR(S)**

Steven Williamson



**7. PERFORMING ORGANIZATION NAME(S) AND ADDRESS(ES)**

Picotronix, Inc.
2553 Bunkerhill, Ann Arbor, MI 48105

**8. PERFORMING ORGANIZATION REPORT NUMBER**

**9. SPONSORING/MONITORING AGENCY NAME(S) AND ADDRESS(ES)**

U. S. Army Research Office
P. O. Box 12211
Research Triangle Park, NC 27709-2211

**10. SPONSORING/MONITORING AGENCY REPORT NUMBER**

ARO 30499.1-EL-SBI

**11. SUPPLEMENTARY NOTES**

The view, opinions and/or findings contained in this report are those of the author(s) and should not be construed as an official Department of the Army position, policy, or decision, unless so designated by other documentation.

**12a. DISTRIBUTION/AVAILABILITY STATEMENT**

Approved for public release; distribution unlimited

**12b. DISTRIBUTION CODE**

93 7 08 038

93-15456

**13. ABSTRACT** *(Maximum 200 words)*

The goal of this Phase I SBIR program was to demonstrate the feasibility and characterize a novel picosecond optical temporal analyzer based on a new 1-ps resolution photodetector. The detector/analyzer system integrates the photodetector on the same chip with a similar laser activated sampling gate. The sensor is called a Sampling Optical Temporal Analyzer, or SOTA.

We have fabricated and tested this device to determine its ultimate speed, sensitivity, and dynamic range. The SOTA's system response was found to be 1.4 ps with a sensitivity of 100 pW. This is the world's fastest, most compact, ultrasensitive, picosecond optical waveform analyzer. It is completely solid-state and has a measured dynamic range of 80 dB.

The potential of this technology for dual-use applications is extensive, reaching into the medical, scientific, optical communications, and automotive industries. The speed, sensitivity, and dynamic range of the SOTA, coupled with its ability to be mass produced using conventional microfabrication, offers us a unique opportunity to develop a new and greatly advanced high speed optoelectronic sensor technology.

**14. SUBJECT TERMS**

Photodetectors, picosecond, optoelectronics, GaAs, imaging, ranging, x-rays

**15. NUMBER OF PAGES**

29

**16. PRICE CODE**

| 17. SECURITY CLASSIFICATION OF REPORT | 18. SECURITY CLASSIFICATION OF THIS PAGE | 19. SECURITY CLASSIFICATION OF ABSTRACT | 20. LIMITATION OF ABSTRACT |
|---|---|---|---|
| UNCLASSIFIED | UNCLASSIFIED | UNCLASSIFIED | UL |

# Novel Solid-State Optical Temporal Analyzer with Picosecond Resolution and Picowatt Sensitivity

**Contract No. DAAL03-92-C-0035**

## FINAL REPORT

Submitted by:



**Picotronix, Inc.**

**P.O. Box 130243**
**Ann Arbor, MI**
**48113-0243**

**30 April 1993**

# Summary of Completed Project

The goal of this Phase I SBIR program was to demonstrate the feasibility and characterize a novel picosecond optical temporal analyzer based on a new 1-picosecond resolution photodetector. The detector/analyzer system integrates the 1-picosecond photodetector on the same chip with a similar 1-picosecond laser activated sampling gate. The sampling gate functions as a dedicated sampling oscilloscope to analyze the electrical signal generated by the photodetector. The output from this device is a quasi-DC current that can be easily measured using conventional electronics. The sensor chip is called a Sampling Optical Temporal Analyzer, or SOTA.

We have fabricated and tested this device to determine its ultimate speed, sensitivity, and dynamic range. The SOTA's system response was found to be 1.4 ps with a sensitivity of 100 pW (noise equivalent power). This is now the world's fastest, most compact, ultrasensitive, picosecond optical waveform analyzer. It is completely solid-state, operates free of jitter and has a measured dynamic range of 80 dB.

The potential of this technology for dual-use applications is extensive and reaches into the medical, scientific, optical communications, and automotive industries. The SOTA represents a major breakthrough in our ability to accurately measure ultrafast optical signals. Its speed, sensitivity, and dynamic range, coupled with its ability to be mass produced using conventional microfabrication, offers us a unique opportunity to develop a new and greatly advanced high speed optoelectronic sensor technology.

TABLE OF CONTENTS

## LIST OF ILLUSTRATIONS

## 1. INTRODUCTION

This report describes the Phase I efforts aimed at developing a novel ultrafast optical sensor. Previous research has shown the feasibility of generating and time-resolving laser-generated picosecond electrical signals using a dual-photoswitch semiconductor correlator.[1] The idea was originally applied to the study of electrical signals propagation on various substrate materials. The goal of this Phase I work was to develop a similar device that would incorporate a new picosecond high-sensitivity photodetector in place of the photoswitches to increase detection sensitivity. The detector/analyzer is called a sampling optical temporal analyzer - SOTA. The enhancement in sensitivity by several orders of magnitude, at virtually no loss in speed, moves the SOTA beyond simply being a spectroscopy technique to being a high-sensitivity optical sensor capable of temporally analyzing picosecond optical signals.

## 2. BACKGROUND

The interest in simple, relatively inexpensive, picosecond detection systems has heightened with the coming of compact picosecond lasers. These lasers will very soon leave the realm of the research laboratory and take their place as fundamental elements of new instrumentation systems. One significant reason for this is the rapid development of highly efficient diode lasers that can be used as pump sources for new picosecond gain media such as optical fibers, or as direct sources of picosecond pulses themselves.

The evolution of picosecond semiconductor[2] and fiber[3] lasers has now reached the point where these systems can produce picosecond pulses at realistically usable energy levels from very compact arrangements. By "compact" we mean lasers sized so they can be integrated as components of other instruments. This also means that within a few years these lasers will be rugged and turn-key, and the instrument users will be blind to their presence within the system. The arrival of this type of compact picosecond laser system in the market place now heralds the need for a simple picosecond detection system so that picosecond sensors and instrumentation can become a reality in the very near future.

Applications for picosecond sensors span many disciplines. We list a few here, including some under development by Picotronix.

Medical

- Picosecond micrometer-resolution laser rangefinder for topographical mapping of the retina for early detection of glaucoma as well as precision feedback during laser-induced sculpting of the eye lens (under development in collaboration with the University of Michigan Ultrafast Science Lab and Kellogg Eye Center).
- Picosecond time-gated imaging for optical detection through turbid media (*ie.* breast tissue, dental material)
- Time-of-flight X-ray 3-D tomography (also applicable to metrology)

Defense/Automotive

- Time-gated laser radar for imaging through fog, haze, *etc.*
- Rapid friend-or-foe or vehicle identification using picosecond time-imaging
- Time-encoded ID labeling for identification of remote objects (*ie.* vehicle ID labeling for law enforcement)

Research

- Time-resolved DNA sequencing
- Picosecond X-ray-to-IR detection and analysis (under development in collaboration with U-M Ultrafast Science Lab)
- Laser synchronization and control sensors (under development in collaboration with MXR, Inc.)

Communications

- Dedicated, cost effective local area network (LAN) picosecond optical time domain reflectometer
- Picosecond optoelectronic logic elements (*ie.* AND-gates and OR-gates) and multi-hundred gigahertz demultiplexers (under development in collaboration with the Photonics Center at Rome Development Labs).

## 3. PHASE I TECHNICAL OBJECTIVES

The main objective of the Phase I project was to demonstrate the feasibility of integrating a picosecond optical detector with a picosecond laser activated sampling gate. Questions to be answered during Phase I were:

- What is the ultimate speed for the SOTA and what is the limiting factor?
- What sensitivity and dynamic range can be achieved?
- What is the relationship between speed and sensitivity?

## 4. DESCRIPTION OF RESEARCH CARRIED OUT

To fulfill our phase I goals we needed to grow GaAs:As epilayers, design an appropriate electrode geometry to assure high speed, characterize the SOTA, and finally demonstrate its utility. We describe each of these areas and offer suggestions for future improvements.

*GaAs:As photoconductors*

The semiconductor material for the SOTA is grown using molecular beam epitaxy (MBE). Unlike conventional MBE, where the substrate temperature is kept between 600° C and 850° C, the growth temperature for our application is more stringent. We need to grow the epilayer at or just a few degrees above the critical temperature for formation of a single-crystal epitaxial layer, that is 190° C to 210° C.

GaAs grown in this temperature range exhibits unusual properties resulting from excess arsenic (~1%).[4] The arsenic is incorporated mainly in interstitials of the crystal, which coalesce into micro-precipitates with a subsequent short-duration high-temperature (600°C) anneal. The most important feature exhibited by GaAs:As is its ultrafast photocarrier lifetime. As we approach the temperature at which polycrystalline GaAs forms the As concentration increases and the carrier lifetime becomes shorter. Carrier lifetimes as short as 0.2 ps have been obtained in material grown at 200°C.[4]

Subpicosecond measurements are made using an all-optical pump-probe technique that measures the change in reflectivity at the surface of a semiconductor.[5] For this experiment, two

150 fs-pulsed laser beams are positioned concentrically on the surface of the GaAs:As epilayer. The larger diameter beam (pump) photogenerates the carriers while the smaller beam (probe) senses the slight difference in reflectivity that results from the plasma-induced change in dielectric constant. The probe pulse is continuously delayed in time to map out the time evolution of carrier generation and recombination/trapping that comprise the material's intrinsic response. Fig. 1 shows the lifetime of the fastest GaAs:As material used for this program. The carrier lifetime is almost as fast as the 150 fs duration pump/probe pulses. The epilayer was grown to a thickness of 1.5 μm at a temperature of 190° C on a (100)-oriented GaAs substrate with a Ga/As flux ratio of 20. After the epitaxial layer was grown it was anneal at 600° C for 10 min. in an As overpressure.

Despite the virtues of GaAs:As, much research is still required to assure quality control. The optimal growth process is not yet known and inconsistencies in temperature calibration between different foundries (and even different machines) exist.

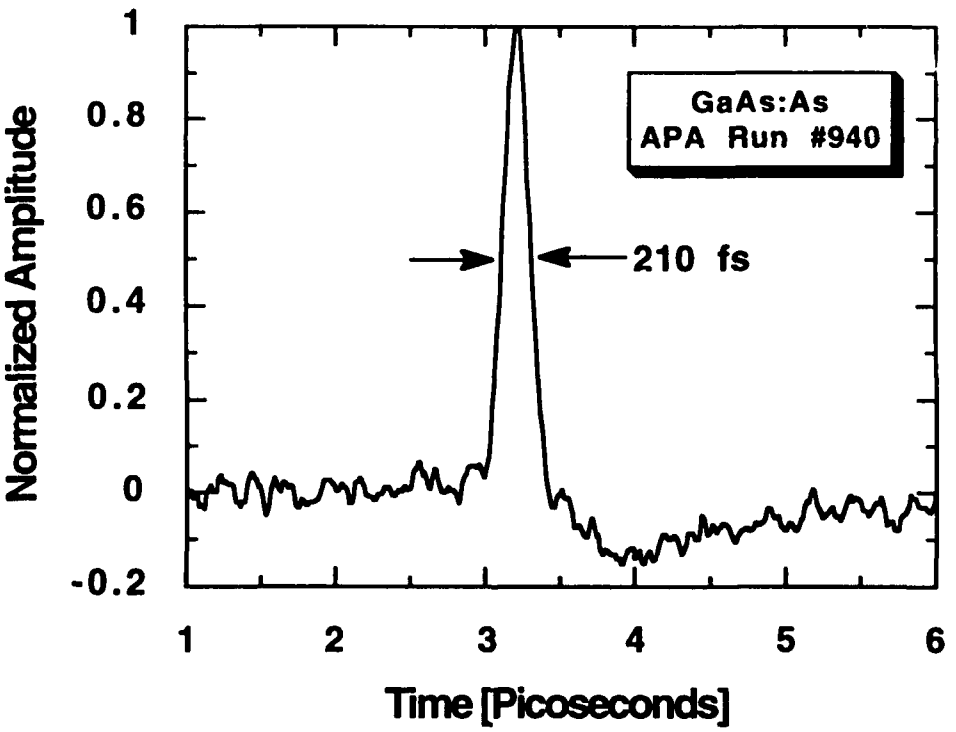


Fig. 1 All-optical time-resolved reflectivity measurement taken of the surface of a GaAs:As epilayer. The 1.5-μm thickness epilayer was grown at 200° C and post annealed at 600° C for 10 min. in an As overpressure. Accurate measurement of the photogenerated carrier density can be made without the need for electrical contacts.

For example, Fig. 2 shows the results of another GaAs:As sample grown presumably under identical conditions by another foundry. The carrier lifetime is 3 ps, over 10 times that found for the previous sample. The problem stems from the need to extrapolate calorimeter data from 500° C down to 200° C. We also must make the assumption that the top surface of the substrate is at the same temperature as the surface contacting the calorimeter. These issues become critical when tolerances of only a few degrees in substrate temperature amount to dramatic changes in material properties.

In addition to subpicosecond carrier lifetime, GaAs:As is also highly resistive ($\geq 10^7$ Ω-cm) and maintains perfect crystallinity as measured using high-resolution TEM and X-ray diffraction.[6] The electron mobility can be as high as 150 $cm^2$/V-s and the dielectric breakdown can exceed 500 kV/cm. The combination of ultrafast carrier lifetime, high mobility, and high resistivity provide the key ingredients for development of ultrafast, high-sensitivity photodetectors.

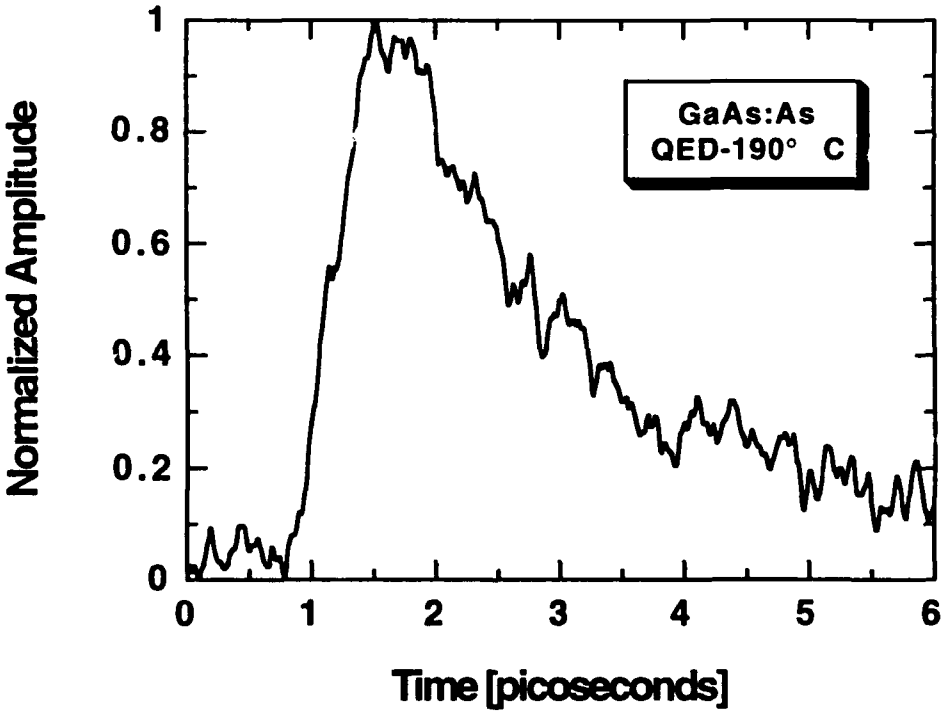


Fig. 2 Reflectivity measurement taken of another GaAs:As grown at a different facility, presumably under the same conditions as the sample used for Fig. 1.

*Detector design*

To take full advantage of these unique properties we need to design the electrode geometry to attain high sensitivity. A detector based on GaAs:As is akin to a photoconductor rather than a photodiode. In a conventional photodiode, a reduction in electrode spacing improves speed with little change in sensitivity. In a photoconductive detector such a reduction increases the sensitivity with little change in speed. Sensitivity for a photoconductor is related to the so-called photocurrent gain, $G=\tau/t_r=\mu_n E/L$. Where, $\tau$ is the carrier lifetime, $t_r$ is the carrier transit time, $\mu_n$ is the electron mobility, E is the electric field, and L is the electrode spacing. Decreasing the carrier transit time across the semiconductor gap to a value comparable to the carrier lifetime increases the photocurrent gain to a value of unity.[7] A photodiode-type detector has an effective gain of unity, regardless of the electrode spacing. For a photoconductor, with a carrier lifetime of 1 ps, this condition is met when the electrode spacing, *i.e.* the actual gap between electrodes, is 0.1 μm.

When optimized, a GaAs:As-based photoconductive detector has the best of both devices, the sensitivity of a photodiode combined with (sub)picosecond intrinsic carrier lifetime of a photoconductor. We achieve this optimal arrangement by using a simple metal-semiconductor-metal (MSM) interdigitated electrode structure with finger spacing and width adjustable down to 0.2 μm.[8] MSM structures could, in principle, be designed for a photocurrent gain greater than unity, making for a detector that exceeds the sensitivity of a photodiode. The need for low-barrier ohmic contacts to permit the injection of new carriers and electrode spacings below 0.1 μm prevent the incremental improvement from being cost effective.

The improvement in sensitivity as functions of electrode spacing and applied bias have been measured. We have fabricated and tested four interdigitated MSM photoconductive detectors of various finger width/spacing. The detectors were fabricated of 300Å/200Å Ti/Au using a JEOL JBX 5DIIF direct-write electron beam lithography system. Each detector has an active area of 50x50 $\mu m^2$ and a finger width/spacing of either 2.0 μm, 1.0 μm, 0.5 μm, or 0.2 μm. In Fig. 3 we show the photomicrograph for the 0.2 μm detector. The large active area assures uniform illumination.

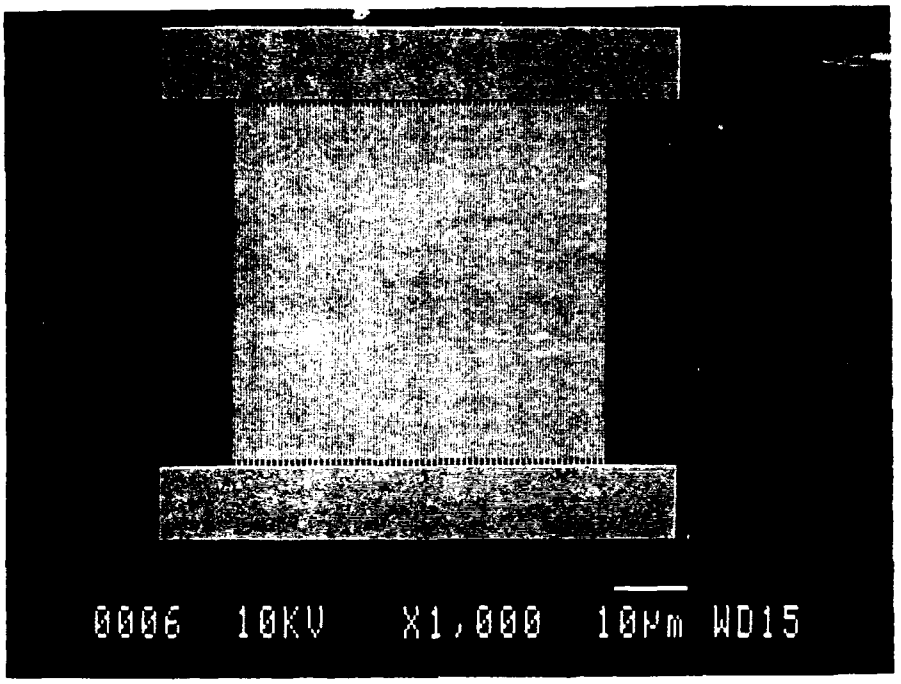


Fig. 3 Photomicrograph of the metal-semiconductor-metal (MSM) photoconductive detector used for measuring the responsivity. Four detectors were fabricated with finger width/spacing of 0.2 µm (shown), 0.5 µm, 1.0 µm, and 2.0 µm. Each has an active area of 50x50 $\mu m^2$.

The I-V curves were measured and plotted in Fig. 4. The values found for the 0.5 µm, 1.0 µm, and 2.0 µm are comparable to dark current densities (current/active area) found with state-of-the-art *p-i-n* photodiodes. The 0.2 µm detector shows considerably higher dark current. For constant electric field, we find the current density for the 0.2 µm detector is, in fact, comparable to the other three. A bias of 8 volts applied to the 0.5-µm detector corresponds to an electric field of 160 kV/cm and produces a dark current density of 32 $pA/\mu m^2$. An electric field of 160 kV/cm across the 0.2-µm detector is obtained with a bias of 3.2 volts, corresponding to a dark current density of 45 $pA/\mu m^2$.

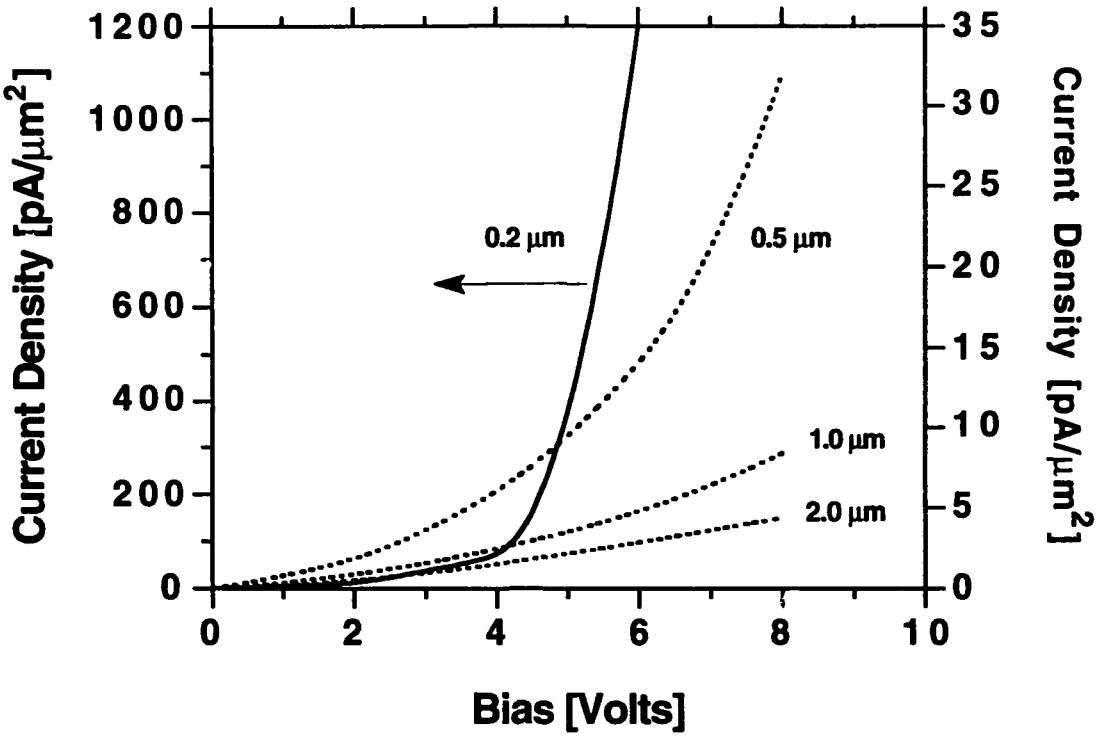


Fig. 4 I-V curves for the four MSM detectors. The dark current density for the 0.2 μm detector is plotted using the left-side ordinate. The remaining three detectors are plotted using the right-side ordinate.

The photocurrent for the four detectors was measured as functions of applied bias and the finger width/spacing. As expected, there is little change in the photocurrent generated as the laser spot size is reduced from 50 μm down to 10 μm. If the applied electric field and the total number of photocarriers is kept constant, the photocurrent generated will also remain constant, independent of the laser spot size. For these experiments we used a HeNe laser focused to 25 μm diameter. Fig. 5 shows the results for two incident power levels. We see that the photocurrent scales nearly linearly with increased bias. We also note a linear increase in photocurrent with decreasing electrode spacing and increasing optical power. With a bias of 6 volts the 0.2 μm detector has a responsivity of 0.1 A/W. These measurements have been made without using AR coatings on the detector or accounting for losses due to metalization (which is avoidable *via* backside illumination). We believe a responsivity exceeding 0.5 A/W is attainable for practical picosecond detectors.

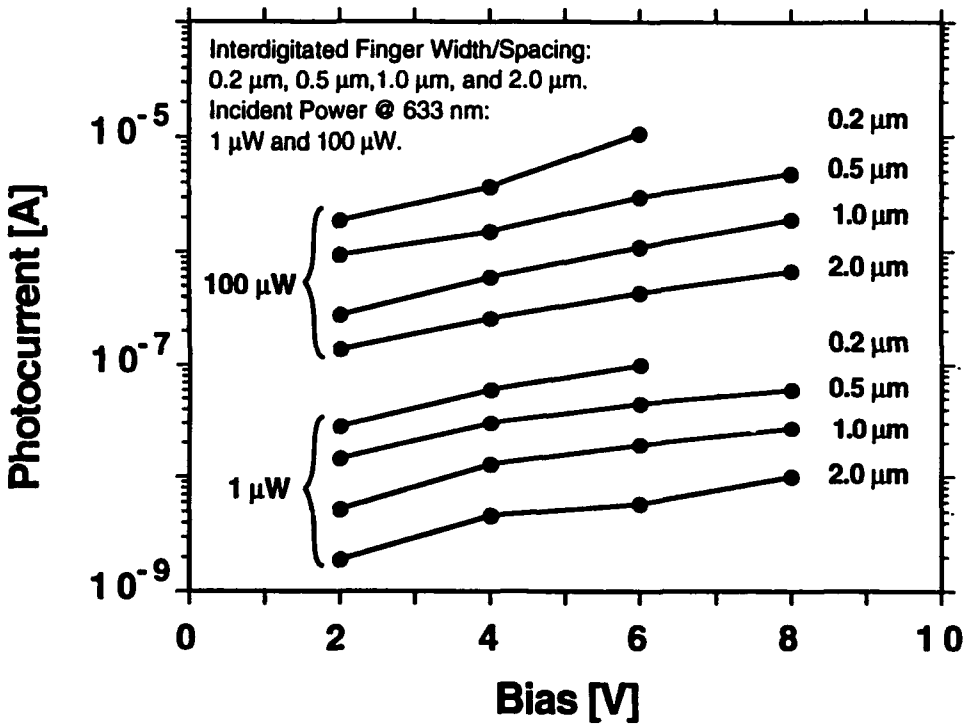


Fig. 5 Photocurrent for the four MSM detectors as a function of the applied bias. The four detectors are plotted at two optical power levels. The 0.2 μm detector biased to 6-V shows a responsivity of 0.1 A/W.

The speed of the detector was previously measured using the technique of electro-optic sampling.[9] A balanced, colliding pulse, mode-locked dye laser operating at 610 nm with a pulse duration of 150 fs and a repetition rate of 100 MHz was used to both excite the detector and probe the signal. Fig. 6 shows the results for the 0.2-μm detector fabricated on GaAs:As with a 0.2 ps carrier lifetime. The speed of the detector is not as fast as the all-optical reflectivity measurement would suggest. The electro-optic probe is partly responsible for the slower than anticipated measurement. A more severe problem exist at the air/dielectric interface. The dielectric mismatch causes the high frequency components of the electrical signal to radiate off the transmission line and into the substrate, reducing the bandwidth of the transmission line signal. This problem can be mitigated either by reducing the transmission line electrode spacing or by eliminating the dielectric mismatch.

Fig. 6 also shows the response of the detector at relatively high pulse energy levels. A 500-fold increase in pulse energy amounts to less than a 20% increase in the response time. If we repeated this picosecond measurement with a conventional photodiode we would find that for pulse energies greater than 0.1 pJ/pulse the detector response rapidly degrades. The photodiode relies on a strong electric field to extract the carriers, where our detector relies on the intrinsic carrier lifetime of the material.

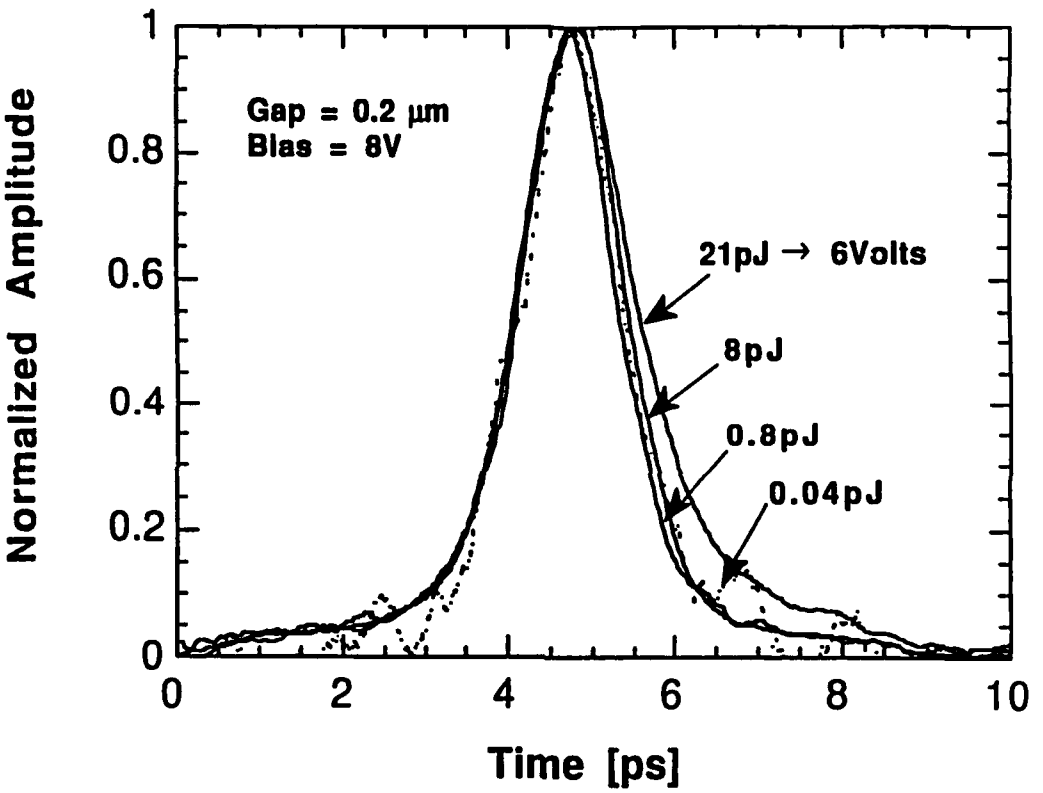


Fig. 6 Set of four signals generated with the 0.2-μm MSM detector. A 500-fold increase in pulse energy amounts to a change in the temporal response from 1.2 ps to 1.5 ps. The measurements were made using the technique of electro-optic sampling.

Fig. 7 summarizes the results for the 0.2-μm detector. Plotted are the photogenerated electrical pulse amplitude and the corresponding on-state conductance of the detector as functions of the pulse energy. For optical pulse energies of 20 pJ the resistance of the detector drops from >10 MΩ down to 30 Ω in 1 ps. This suggest that one photoconductive detector can function either as a picosecond detector or a picosecond gate, according to the incident pulse energy. This dual-function photoelement gives the SOTA its unprecedented performance.

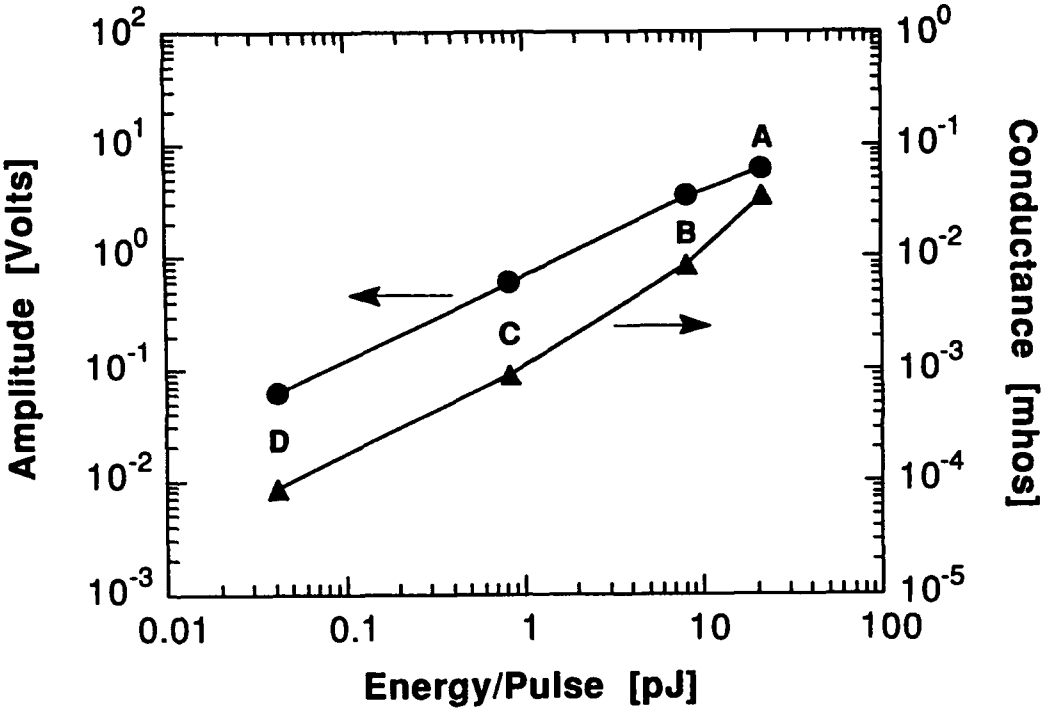


Fig. 7 Peak amplitude and conductance of the signals shown in Fig. 6 plotted against the incident pulse energy. This plot highlites the dual functionality essential for the SOTA.

*SOTA design*

The best performance to date for the SOTA incorporates the same coplanar transmission line structure first developed to characterize the fast photodetectors. This configuration, shown in Fig. 8, integrates the interdigitated MSM photodetector into the coplanar transmission line and assures good coupling of the electrical signal to the propagating mode and also eliminates the possibility of parasitic losses from wire bonds and bonding pads. A voltage is applied across the two electrodes and adjacent fingers of the detector. Two SOTA designs were fabricated with the finger width/spacing of 0.2 μm or 1.0 μm, with the detector and gate areas fixed at $10 \times 10\ \mu m^2$. An optical signal on the detector initiates a current transient that generates an electrical replica. The electrical signal propagates in both directions away from the detector along the transmission line.

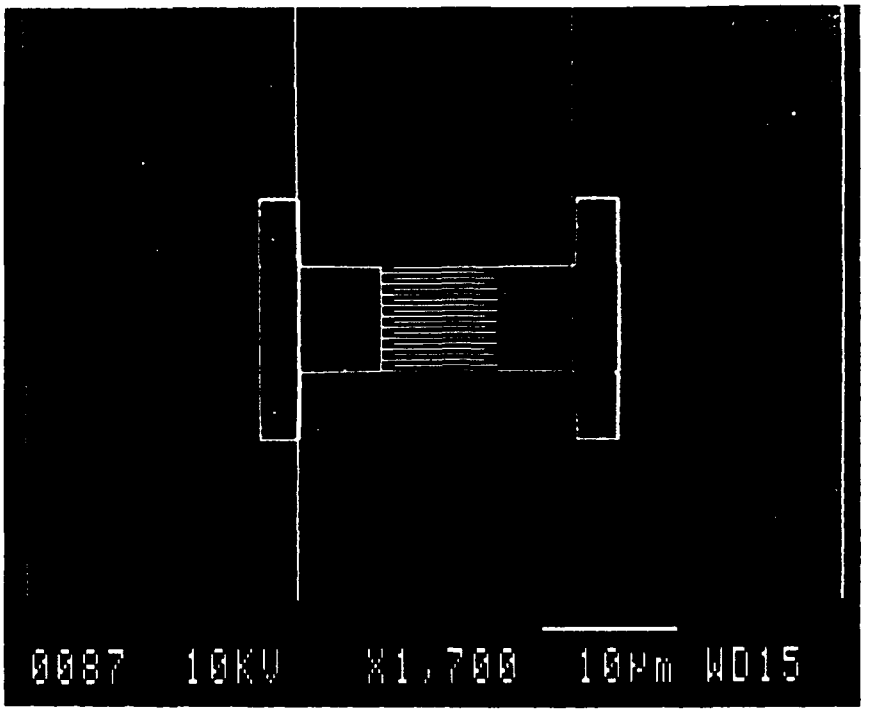


Fig. 8 The 0.2-µm MSM detector mounted between the coplanar transmission line electrodes. The signal generated is launched in both directions away from the detector. The detector was integrated into the transmission line to eliminate distortions from parasitics.

To reduce dark current, a 100-nm thickness layer of SiO is deposited to separate the transmission line electrodes from the GaAs. Fig. 9 shows a typical photogate with the SiO layer in place and a window, through which electrical contact is made by the interdigitated fingers. This technique also prevents any interference by photocarriers generated outside the detector region. This is especially important for the sampling gate, which is activated by an energetic gate pulse and is only 10 µm from the biased transmission line electrodes. With the SiO buffer in place virtually no current can be generated by misdirected light.

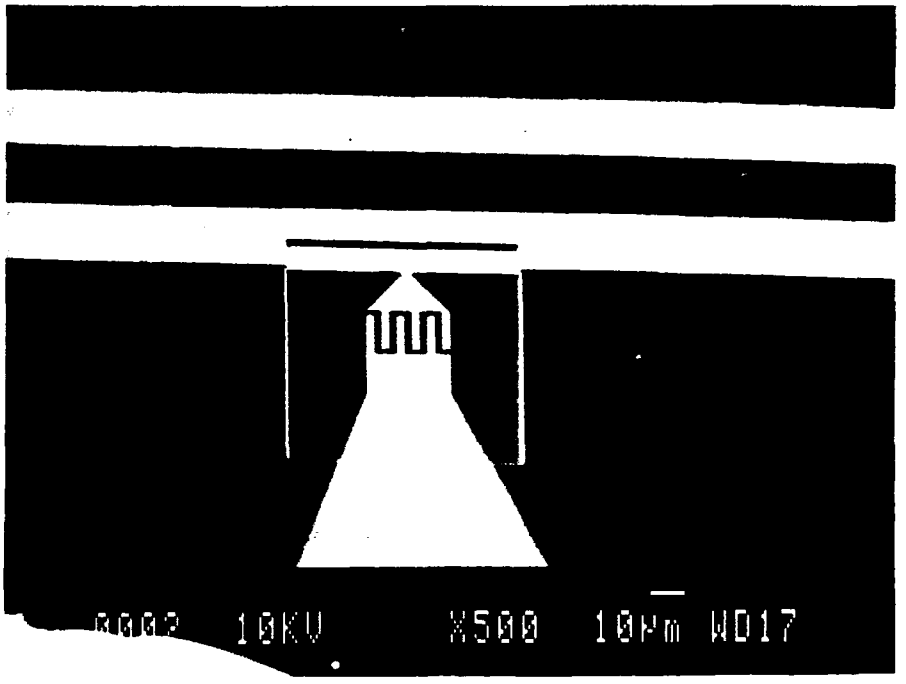


Fig. 9 The sampling gate of the SOTA is positioned 200 µm away from the detector on the ground electrode of the transmission line. The SiO window separates the metalization from the semiconductor everywhere except at the gate.

Fig. 10 graphically depicts the experimental layout for the SOTA. The sampling gate is positioned 200 µm from the detector, or approximately 2 ps in propagation time, and connected to the ground electrode of the transmission line. The distance between the detector and gate is kept short to reduce dispersion. The gate electrode is normal to the transmission lines for a distance of 3 mm to avoid any rf coupling. When the gate is activated its resistance drops below 100 Ω and current from the ground electrode transfers across the gate. The sampled signal is effectively mixed down to quasi-DC frequencies and can than be measured using conventional electronics. In fact, a portable digital voltmeter can measure the signal directly. To map out the entire electrical signal (*ie.* optical replica), we introduce a delay between the the gate pulse and optical signal to sample each slice of time. Recently, we have shown that rapid scanning of the relative delay is also possible and offers the user the ability to "see" the optical event in real time.

Fig. 11 is a photomicrograph of the actual SOTA device. The matrix in the middle of the pattern is a set of two rows of 50x50 $\mu m^2$ photodetectors used for the sensitivity measurements discussed earlier. (We omitted the fifth detector, with finger width/spacing of 0.1 μm, from our results due to inconsistencies in the data). From this photomicrograph we gain an appreciation for the size of the 10x10 $\mu m^2$ detector and gate. These dimensions are required to hold the rc time constant to less than 1 ps. A 0.2 μm detector of this size has a capacitance of 4 fF. When integrated into a 90 Ω impedance transmission line the theoretical response is 360 fs. We will propose, as part of our Phase II program, to develop a novel electrode geometry than can maintain the high sensitivity and picosecond speeds with a detector size of 100x100 $\mu m^2$, and possibly as large as 1x1 $mm^2$.

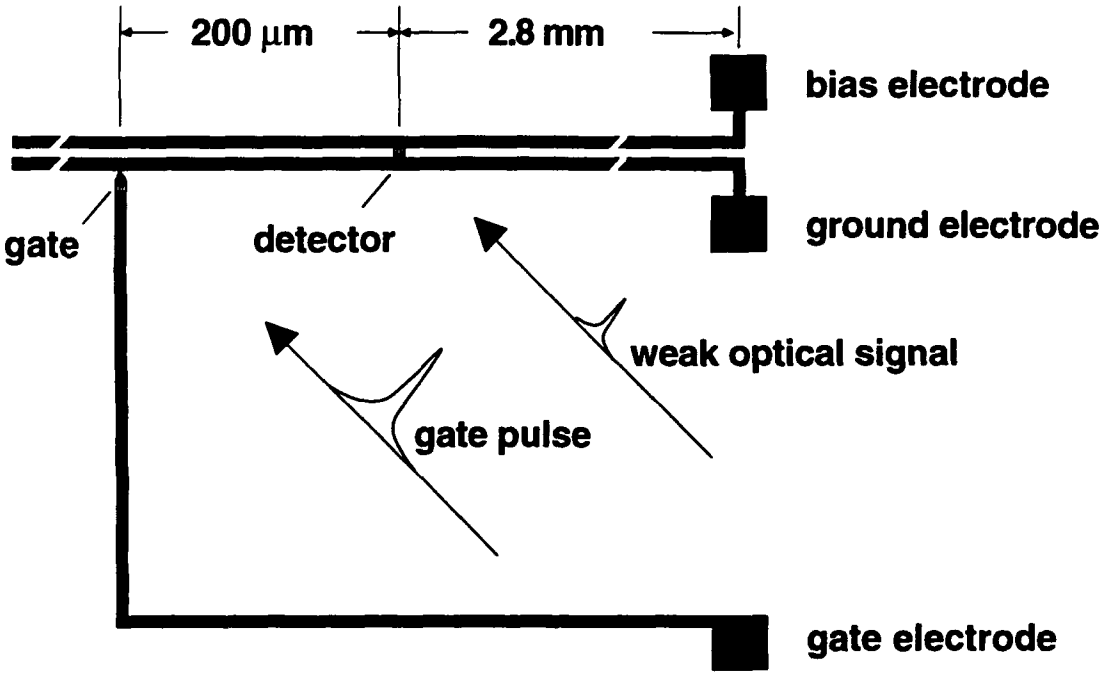


Fig. 10 Fabrication layout for the SOTA. The 200 μm distance between the detector and gate amounts to a propagation time of 2 ps. The first reflection that returns from the end of the transmission line takes 60 ps to arrive at the gate.

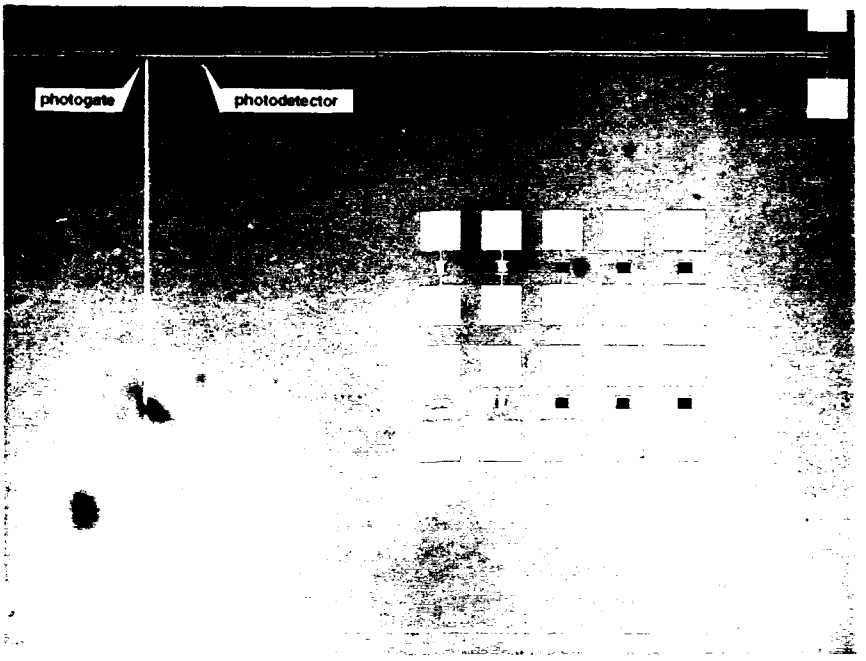


Fig. 11 Photomicrograph of the actual SOTA layout. The matrix of patterns in the center are the 50x50 $\mu m^2$ detectors used earlier for measuring the responsivity (shown in Fig. 3).

Instead of wire bonding individual SOTAs for testing, we opted for leaving the SOTAs on the wafer and making electrical contact using mechanical probes. Fig. 12 is a photograph of the actual experimental apparatus. The mechanical probes and the stage holding the wafer are designed to move independent of one another. This setup greatly speeds the testing process and enables quick isolation to prevent electro-static discharge. The signal gated to the gate electrode is sent to high gain current preamplifier and lock-in amplifier. The lock-in is tuned to a specific frequency, which is also the frequency at which the optical signal under study is being modulated. Amplitude modulation of this signal is accomplished using a mechanical chopper placed in the beam. The lock-in amplifier filters all signals except those having the precise frequency and phase of the mechanical chopper.

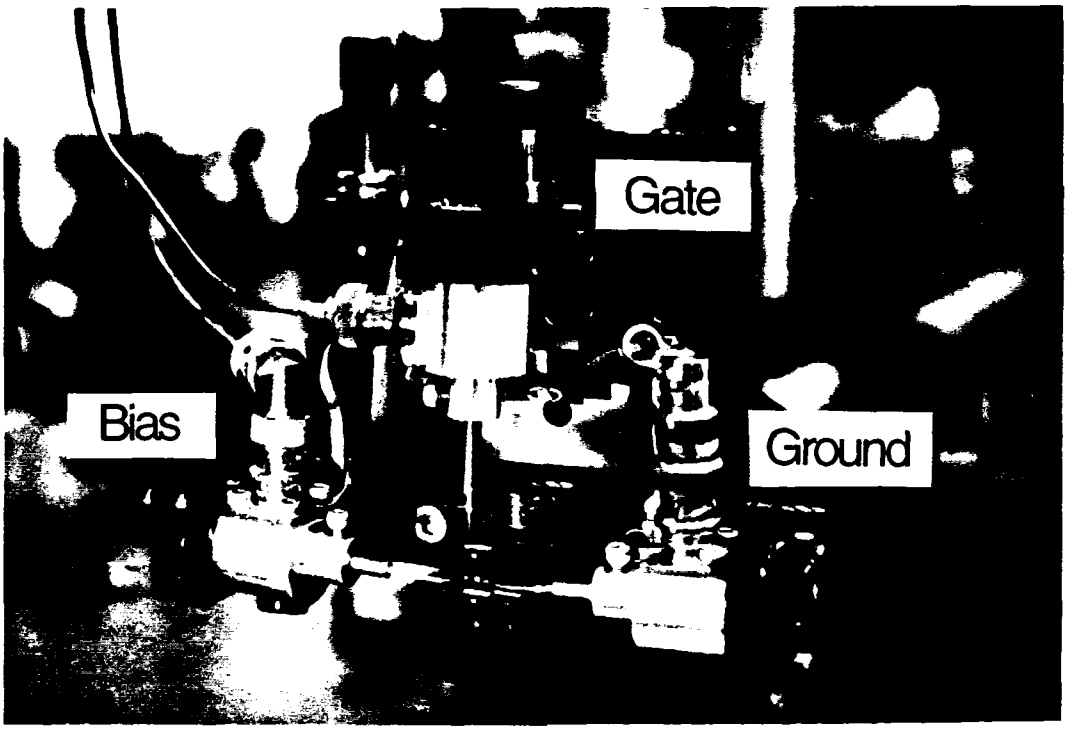


Fig. 12 Experimental apparatus for testing the SOTA. The bias, gate, and ground probes make contact to their respective bond pads (shown in Fig. 1).

## 5. RESULTS

*Temporal response of the SOTA*

Fig. 13 shows the system response for the SOTA. The measurement was made with the optical signals incident on the detector and gate both being of 150 fs duration. The response of the SOTA is 1.4 ps. This the fastest, high sensitivity detector/analyzer in the world. The deconvoluted speed of either the detector or gate is 1.0 ps.

We see that the response is not symmetric, indicating the SOTA is in fact not behaving like an ideal autocorrelator. The tail shown on the trailing side of the pulse persists for 30 ps. The tail results from a combination of capacitive and inductive reactance that couples charge through the

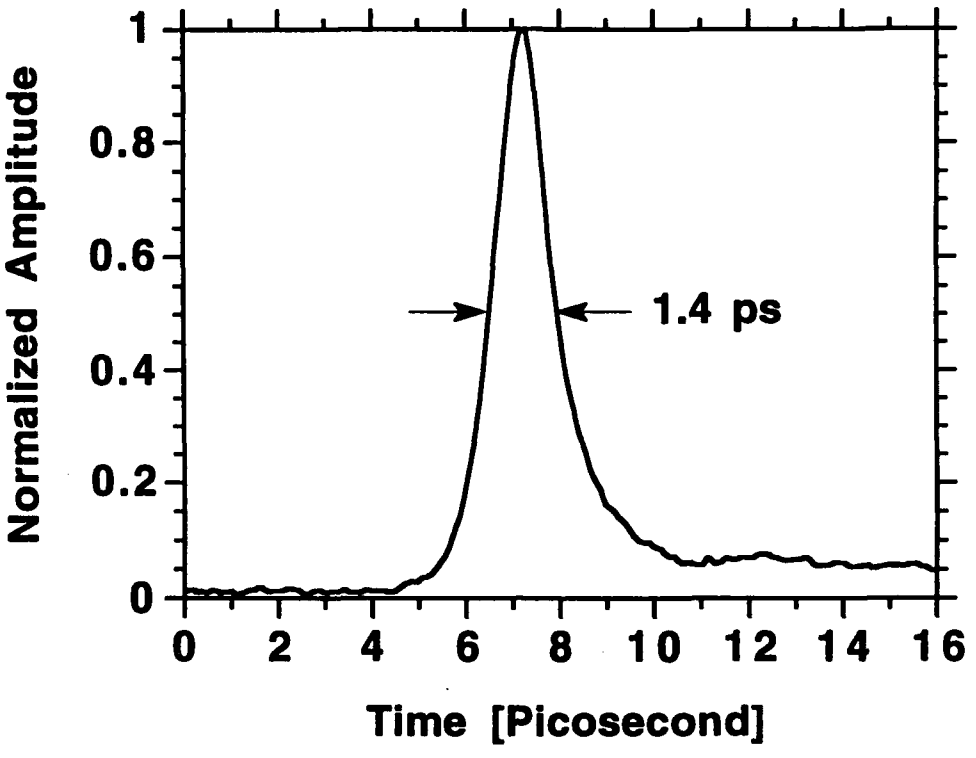


Fig. 13 Temporal response of the SOTA.

interdigitated sampling gate and onto the gate electrode. The net charge is zero and is transferred without the need of the optical gate pulse. When the optical pulse does arrive, say 10 ps after the electrical pulse has past, the gate electrode is still residually charged with a rapidly decaying bipolar pulse. The gate electrode is not of constant impedance and effectively reflects the coupled signal, in a backward-propagating mode, onto the gate.

Activating the gate then transfers charge *off the gate electrode* and onto the ground electrode, appearing as though charge is being transferred onto the gate electrode. Our lock-in amplifier cannot tell which direction charge is transferred. It only filters and amplifies signals that are produced by the *combined* action of detection and gating, via the technique of difference-frequency mixing. Charge that is reactively-coupled onto the gate electrode will not necessarily be amplified by the lock-in. Only coupled charge that is subsequently gated back to the transmission line, due to the presence of the optical gate pulse, will be properly filtered and amplified by the lock-in. After 30 ps this displacement current pulse decays away, with no net effect on the balance

of charge. Only through the process of mixing at our photogate is the signal revealed. The tail can be greatly reduced by using a straight gap (not interdigitated) for the sampling gate to reduce the reactance. The gate pulse is always coherent and thus can be focused to 1 μm or less, therefore allowing small gaps to be used.

The fact that the leading edge of the response is flat and holds to the baseline indicates that the GaAs:As indeed has an extremely fast carrier lifetime and no residual tail. During our Phase II we will address this problem of asymmetry.

*Sensitivity of the SOTA*

We have succeeded in pushing the sensitivity of the SOTA to 100 pW (NEP). The gate pulse energy for this result was 10 pJ. The useful dynamic range now extends from an average power of 100 pW to 10 mW, or 80 dB. A dynamic range of 80 dB surpasses by a factor of a 1000 the state-of-the-art in streak camera technology. Although the sensitivity is now comparable to the streak camera, it still remains 2 orders of magnitude away from the Johnson noise limit of 1 pW. We are now limited by laser noise fluctuations. Instabilities in the amplitude and beam position are responsible for the existing noise. Our colliding pulse mode-locked laser has 10% amplitude ripple and is prone to slight beam movement, caused by the use of two intercavity dye jets. The problem actually stems from the Schottky barriers that form the MSM contacts of the gate. The barrier at the junction has an internal electric field that permanently biases the gate to a few hundred millivolts. The intense gate pulse can generate an electrical signal as large as 100 mV in amplitude.

What makes the interdigitated gates unique is the alternating polarity of the electric field between adjacent fingers. Photovoltaic current generates opposing electrical signals that effectively cancel one another. However, when the electrical signal being sampled is as weak as 1 pA, residual current generated at the gate does become significant. Discrimination *via* the lock-in by tuning away from the modulated (chopping) frequency of gate signal and to the sum frequency of the gate + detector signal can eliminate a great deal of this background signal. Unfortunately, if the gate signal fluctuates too much, the signal is no longer of narrow bandwidth centered at the modulated frequency and can generate a sizable signal at the sum frequency. A similar noise contribution can also be generated by the micromotion of the gate beam across the gate.

We can address this problem either by reducing the laser noise or by designing a gate that is impervious to laser fluctuations. The new picosecond sources now becoming available have significantly lower noise levels. As for redesigning the gate, we will begin by replacing the

Schottky contact that forms the metal-semiconductor interface with an ohmic contact. This should greatly reduce the photovoltaic contribution from the gate. Since both the amplitude fluctuations and beam movement occur on the microsecond time scale, we can also introduce a feedback loop to cancel the photovoltaic signal. This would be accomplished by adjusting a voltage applied to the gate which is equal in amplitude but opposite in sign to its photovoltaic counterpart.

Another approach to improving sensitivity is to simply increase the gate pulse energy. To test this idea we increased the gate energy from 10 pJ/pulse to 70 pJ/pulse. This is sufficient to drive the gate below 10 Ω. The lower the gate resistance the higher the signal-to-noise. But there is a limit to how low the gate resistance can be made before the gate begins to saturate and the response time degrades. At 70 pJ/pulse, the response time increased by 40%. There are not many trades available to us that will allow a reduction in the gate resistance to ≤ 10 Ω and also attain a single-picosecond response. For picosecond response times we are restricted to a gate size no greater than 10x10 $\mu m^2$. We will propose as part of our Phase II program a technique that will enable both higher sensitivity and speed to occur simultaneously.

*Applications*

We have pursued two new applications for the SOTA. The first is an ultrahigh resolution profilometry technique. There is a growing need in the field of optometry to make precise topographical measurements of the retina to identify early signs of glaucoma. The techniques now available lack the depth resolution needed to resolve below 100 μm. The requirement that the incident light level be eye safe added to the ambiguity that results for multiple reflections from the lens precludes the possibility of routine testing. By time resolving the return signal we not only measure the range with micrometer resolution but we can also time window away erroneous reflections resulting from each interface in the eye. Fig. 14 shows a simple experiment conducted to show the resolution possible using a hard surface. The object to be scanned is the serrated edge of a U.S. quarter. The laser is focused to a 10 μm spot and is scanned by translating the quarter. Fig. 15 shows the results. We can see clearly the ridges with resolution of the order of 50 μm. We can also see that the curvature of the quarter. The average power of light returning to the SOTA detector was less than 1 μW. The combined detection sensitivity and speed of the SOTA uniquely qualifies it for this kind of application.

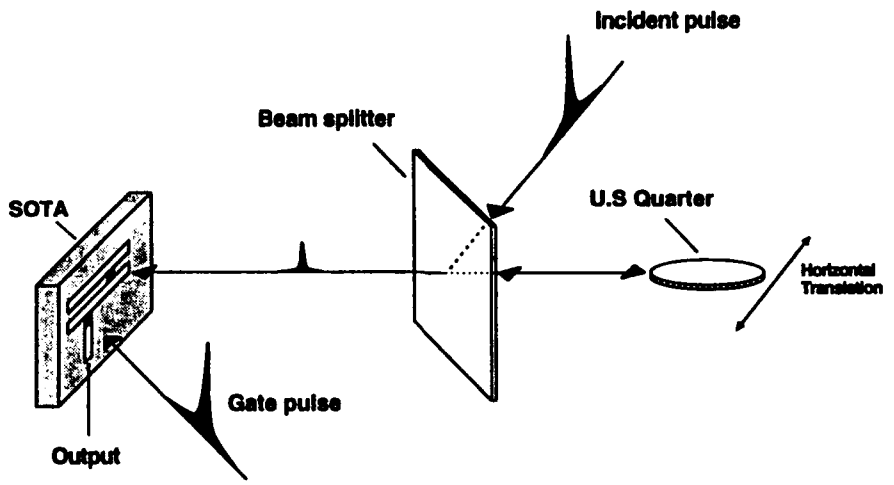


Fig. 14 Experimental setup for micrometer-resolution rangefinding. The object being scanned is the serrated edge of a U.S. quarter.

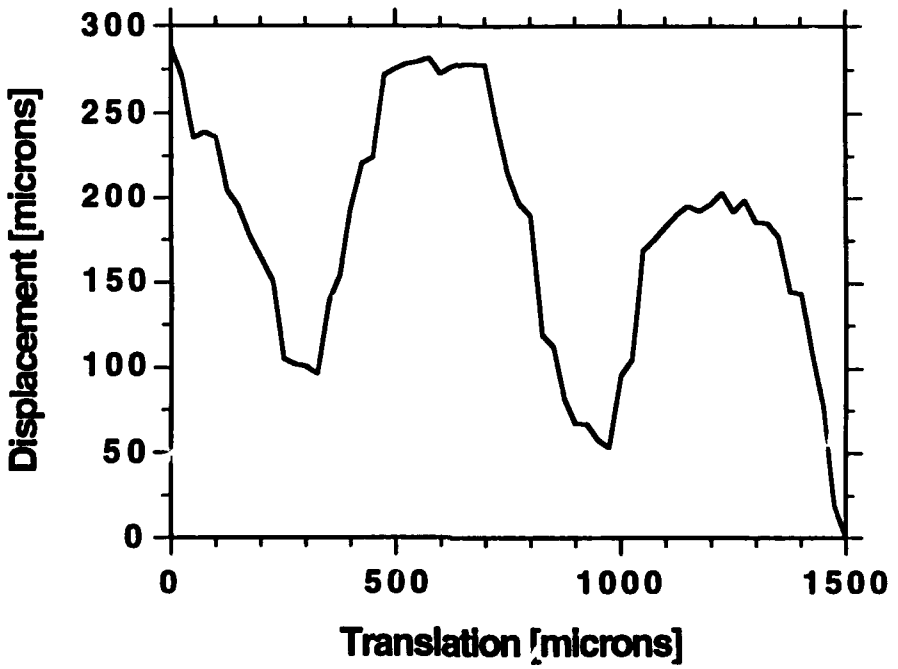


Fig. 15 Measured depth profile of the ridges that form the edge of a quarter. Features in the profile of less than 50 μm are measurable.

A second ranging experiment was performed. Here, we are not so interested in the absolute range off a hard surface as we are with the spacing of a stack of partially-reflective mirrors positioned along the beam's path. The application we envision is ID labeling along the lines of bar coding only now the information is encoded along the Z- or time-axis. This technique will have utility for those applications where the encoded label cannot be scanned in the near field. Unlike with the conventional bar code, where the distance between the scanner and laser is kept short, the 'temporal bar code' operates independent of distance to the extent that the signal-to-noise of the return signal is adequate. Spatially-stored information with resolution of the order of a UPI label becomes impossible to read beyond a few meters without the aid of a telescope. Information stored in the time domain remains invariant with distance, provided a detection system is available to time resolve the information. The SOTA is the ideal detector for this application. With 1-ps resolution, mirror spacings as close as a few hundred micrometers can be resolved. Also, the high dynamic range offered by the SOTA permits many mirrors to be stacked together to increase the information density.

Fig. 16 shows the experimental setup used to demonstrate this concept. For the initial experiment the mirrors are glass microscope slides. There are five mirrors or bits of information that form the code, corresponding to $2^5$ (32) possible code numbers. The mirrors are equally spaced. Two measurements are made, the first with all five mirrors in placed and the second with the second mirror in the stack removed. Fig. 17 shows the results of these two configurations. We see that the second pulse is clearly missing from the train (bottom trace).

Possible applications for time-encoded labeling include law enforcement (particularly automotive and recreational boating industries), remote identification of infantry and vehicles in the field, and management of trains, ships, live stock, *etc.* In principle, tens of mirrors could be stacked together as an integral part of a cube corner retroreflector. This configuration reflects the beam back onto itself and returns it collimated directly back to the SOTA. Many other applications for this technique will emerge as we further the development of the SOTA during our Phase II.

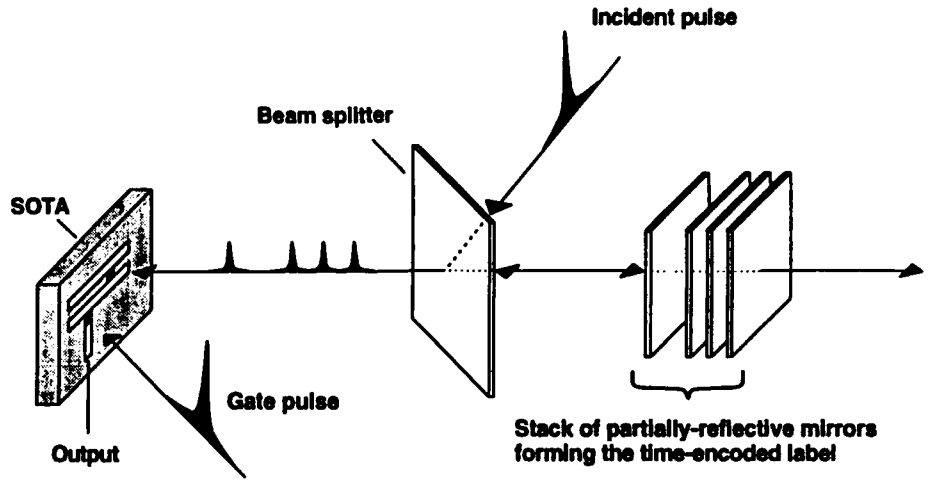


Fig. 16 Experimental setup for demonstrating a new technique to time encode information. The incident optical pulse passes through a stack of partially-reflective mirrors. The reflected signal is a sequence of pulses, representing the relative spacings between the mirrors. The SOTA is sufficiently fast and sensitive to measure the encoded information.

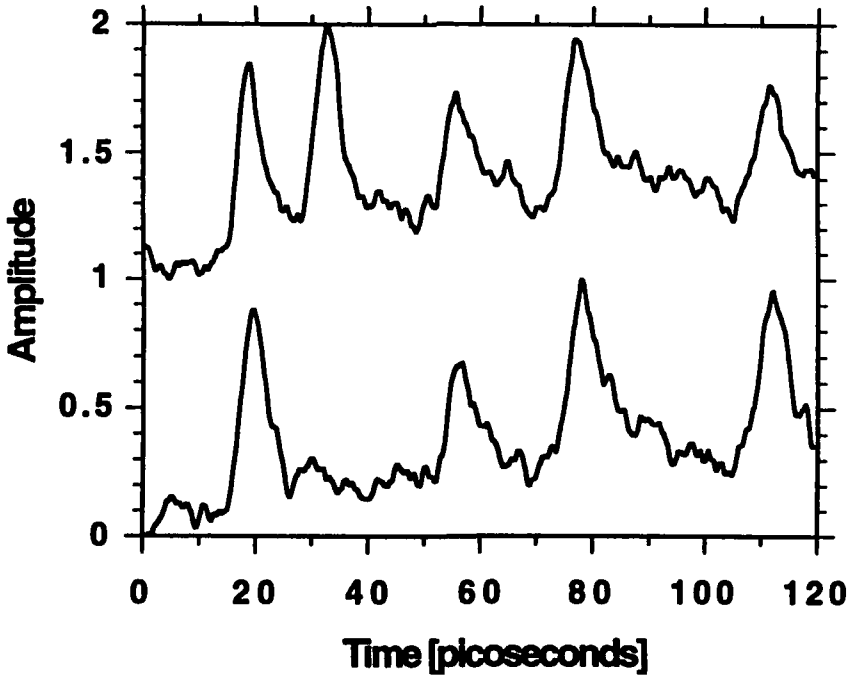


Fig. 17 Result of the temporal 'bar code'. The top trace shows five pulses, representing reflected signals from five mirrors. The bottom trace represents the mirror arrangement depicted in Fig. 16. The second mirror was removed, causing the second pulse in the encoded train to be deleted.

## 6. CONCLUSIONS

The phase I program has been highly successful. We have developed a novel all-solid-state optical detector and integrated analyzer that combine to form the world's fastest, most compact, ultrasensitive, picosecond optical waveform analyzer. The output from this device is a quasi-DC current that can be measured using conventional electronics. The speed, sensitivity, and dynamic range of the SOTA, coupled with its ability to be mass produced using conventional microfabrication, offers us a unique opportunity to develop a new and greatly advanced generation of ultrafast optoelectronic technology.

The primary focus for the Phase II centers on developing larger active area detectors to collect more light and also to push the speed and sensitivity to the theoretical limits. Concurrent to this effort, we will be working on improving quality control of the GaAs:As growth procedure and pursuing the development of long-wavelength photoconductors for application with optical communications.

## 7. REFERENCES


1. M.B. Ketchen, *et.al.*, Appl. Phys. Lett., **48**, 753, 1986.
2. L.Y. Pang, *et al.*, "High-power modelocked diode array using intracavity nonlinearity", Paper JThB4, Proc. Conf. on Lasers and Electro Optics, Anaheim, CA, 1992.
3. K.V. Reddy, *et al.*, "A turn-key 1.5μm picosecond Er/Yb fiber laser", Postdeadline paper PD-17, Proc. OFC/IOOC Conf., San Jose, CA, 1993.
4. F.W. Smith *et al.*, IEEE Electron Dev. Lett. 9, 77, 1988.
5. S. Gupta, Ph.D thesis, Univ. of Michigan, Ann Arbor, MI, 1992.
6. F.W Smith, Ph.D thesis, Massachusetts Institute of Technology, Cambridge, MA, 1990.
7. S.M. Sze, *Physics of Semiconductor Devices*, 2nd.ed., 746, (Wiley, NY, 1981)
8. Y. Chen *et al.*, Appl. Phys. Lett., **59**, 16, 1986, 1991.
9. J.F. Whitaker, *et al.*, Microelectron. Eng. **12**, 369, 1990.